BIOCHEMISTRY
including biophysical chemistry & molecular biology

Article

pubs.acs.org/biochemistry

Characterization of Two Quinone Radicals in the NADH:Ubiquinone Oxidoreductase from *Escherichia coli* by a Combined Fluorescence Spectroscopic and Electrochemical Approach

Ruth Hielscher,[†,§] Michelle Yegres,[†] Mariana Voicescu,[†,∥] Emmanuel Gnandt,[‡] Thorsten Friedrich,[‡] and Petra Hellwig*[,†]

[†]Laboratoire de bioelectrochimie et spectroscopie, UMR 7140, CNRS, Université de Strasbourg, 1, rue Blaise Pascal, 67070 Strasbourg, France

[‡]Institut für Biochemie, Albert-Ludwigs-Universität, Albertstraße 21, 79104 Freiburg, Germany

ABSTRACT: The NADH:ubiquinone oxidoreductase (complex I) couples the transfer of electrons from NADH to ubiquinone with the translocation of protons across the membrane. It was proposed that the electron transfer involves quinoid groups localized at the end of the electron transfer chain. To identify these groups, fluorescence excitation and emission spectra of *Escherichia coli* complex I and its fragments, namely, the NADH dehydrogenase fragment containing the flavin mononucleotide and six iron−sulfur (Fe−S) clusters, and the quinone reductase fragment containing three Fe−S clusters were measured. Signals sensitive to reduction by either NADH or dithionite were detected within the complex and the quinone reductase fragment and attributed to the redox transition of protonated ubiquinone radicals. A fluorescence spectroscopic electrochemical redox titration revealed midpoint potentials of −37 and− 235 mV (vs the standard hydrogen electrode) for the redox transitions of the quinone radicals in complex I at pH 6 with an absorption around 325 nm and a fluorescence emission at 460/475 nm. The role of these cofactor(s) for electron transfer is discussed.

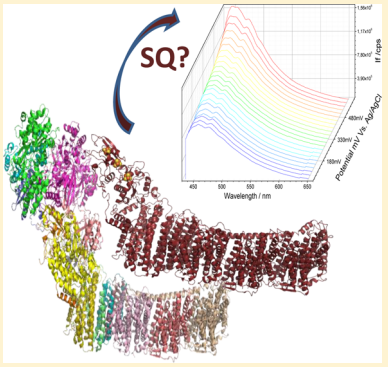

The proton-pumping NADH:ubiquinone oxidoreductase, also known as respiratory complex I, is involved in cellular respiration by coupling electron transfer from NADH to ubiquinone with the translocation of protons across the membrane according to the overall equation

$$NADH + Q + 5H^+_n \rightarrow NAD^+ + QH_2 + 4H^+_p$$

where Q refers to ubiquinone and H^+_n and H^+_p refer to the protons taken up from the negative inner and delivered to the positive outer side of the membrane, respectively.[1−3] Mitochondrial complex I from bovine heart consists of 45 different subunits and contains one flavin mononucleotide (FMN) and eight iron−sulfur (Fe−S) clusters as cofactors.[4,5] The mitochondrial complex has a mass of ∼980 kDa. Bacterial complex I typically consists of 14 subunits that add up to a mass of ∼550 kDa.[6,7] The bacterial complex contains the same cofactors as the mitochondrial one and is sensitive to the same inhibitors. Bacterial complex I is considered to be a minimal structural form of an energy-converting NADH:ubiquinone oxidoreductase.[6,8] Electron microscopy revealed the two-part structure of the complex consisting of a peripheral arm and a membrane arm.[9−11] In bacteria, seven globular subunits containing the binding sites for NADH, FMN, and the Fe−S clusters build up the peripheral arm.[6,12,13] The membrane arm consists of the seven residual polytopic proteins forming 64 transmembrane α-helices.[11] The arm most likely participates in quinone binding and is involved in proton translocation.[8,14−16] Thus, the electron transfer reaction is spatially separated from the proton translocation reaction. Most likely, these processes are coupled by conformational changes. This proposal was supported by the X-ray structures of bacterial complex I from *Thermus thermophilus* at a resolution of 3.3 Å[17−19] and the mitochondrial complex from *Yarrowia lipolytica* at a resolution of 6.3 Å.[20,21]

Escherichia coli complex I contains 13 different subunits [NuoA−NuoN (from NADH:ubiquinone oxidoreductase)]. The primary electron acceptor FMN accepts a hydride from NADH. The electrons are transferred further to the substrate ubiquinone by a chain of seven Fe−S clusters [N3, N1b, N4, N5, N6a, N6b, and N2 (nomenclature of Ohnishi)]. An additional cluster (N7) found in some species is not involved in the electron transfer reaction but was shown to be essential for the stability of the complex.[22] The fact that Fe−S cluster N1a is not directly involved in the transfer of the electron to the quinone and acts as an antioxidant to prevent the formation of reactive oxygen species (ROS) has been discussed.[23]

The mechanism of quinone reduction is not known. As Fe−S clusters are one-electron donors and the quinone is a two-electron acceptor, a sequential reduction of the substrate by the most distal Fe−S cluster N2 would lead to the formation of a

Received: July 24, 2013
Revised: November 19, 2013
Published: November 26, 2013

quinone radical. If not tightly bound by the protein, this radical might escape the complex and contribute to the production of ROS. Two quinone radicals have been detected during turnover of the complex.[24−26] These radicals seem to be essential for the enzyme's mechanism; the molecular identity of these radicals remained unclear. The presence of an additional, quinoid-type cofactor probably involved in quinone reduction was previously suggested on the basis of UV−vis, EPR, and Fourier transform infrared spectroscopy experiments.[27,28] Preparations of mitochondrial complex I from *Neurospora crassa* and the bacterial form from *E. coli* were spectroscopically analyzed under anaerobic conditions in various redox states. UV−vis redox difference spectra were obtained that derived neither from the FMN nor from the EPR-detectable Fe−S clusters. The midpoint potential of this group was determined to be approximately −100 mV [vs the standard hydrogen electrode (SHE)]. Here, we use fluorescence spectroscopy and electrochemistry to substantiate the presence of quinoid cofactors in complex I.

MATERIALS AND METHODS

Sample Preparation. Complex I was prepared by affinity chromatography from overproducing *E. coli* strain ANN0221/pBAD*nuo*/*nuo*F_{His} as described previously.[29] The overproduced NADH dehydrogenase fragment consisting of subunits NuoE, NuoF, and NuoG was prepared from *E. coli* strain BL21(DE3)/pET11a/*nuo*B-G/NuoF_C as described previously.[30,31] The quinone reductase fragment consisting of all complex I subunits but NuoE, NuoF, and NuoG was obtained by alkaline treatment of the complex as previously reported.[10] All chromatography steps were conducted at 4 °C. The samples were concentrated by ultrafiltration (100 kDa molecular mass cutoff, Amicon, Millipore), shock-frozen in liquid nitrogen, and stored at −80 °C until they were used. The samples were concentrated as approximately 200 μM stock solutions. Prior to the measurements, 4 μL aliquots were diluted with 50 mM MES-NaOH, 50 mM NaCl, and 0.1% (w/v) dodecyl maltoside (pH 6.0) to a final concentration of 2 μM. NADH (Sigma-Aldrich) was added to final concentrations of 0.5, 1, and 2 mM. Alternatively, samples were reduced by addition of 1 mM dithionite. Ubiquinone-10 was purchased from Sigma-Aldrich. A 1 mM solution in CH_3CN (electrochemical grade) was used, and $TBAPF_6$ (was recrystallized) was also from Sigma-Aldrich.

Steady-State Fluorescence Spectroscopy. The fluorescence emission and excitation spectra were recorded with a Fluorolog FL3-22 instrument equipped with a 450 W xenon lamp and a TBX 04 detector (Horiba Jobin Yvon), using 5 nm bandpasses for the excitation and emission monochromators, increments of 1 nm for the emission monochromator, and integration times of 0.1 s. The excitation wavelengths were 295 nm (Trp contribution), 365 nm (FMN contribution), and 420 nm (other chromophores). The emission wavelengths were 470 and 532 nm.

Electrochemically Induced Fluorescence Spectroscopy. For the electrochemically induced fluorescence studies, a spectroelectrochemical thin layer cell adapted for usage in the front-face fluorescence modulus is used as described recently.[32] A 10 nm bandpass monochromator was used for the excitation and a 5 nm bandpass for the emission. The increment for the emission monochromator was 1 nm and the integration time 1 s. The excitation wavelength was 365 nm. All fluorescence measurements were performed at 10 °C, and the emission spectra were corrected for the lamp, the monochromator, and the detector response.

Electrochemistry. The ultra-thin layer spectroelectrochemical cell with the path length set to 6−8 μm for the fluorescence was used as previously described.[32−35] To prevent protein denaturation, the gold grid working electrode was chemically modified with a solution containing 2 mM cysteamine.[34,35] The gold grid was incubated for 30 min in the solution and washed with distilled water. To accelerate the redox reaction, mediators were used at a final concentration of 45 μM each as described previously.[34] At the given concentrations and with a path length of <10 μm, no spectral contributions from the mediators in the emission spectra and with the giving excitation wavelength were detected in control experiments with samples lacking the protein. Approximately 6−7 μL of the protein solution was sufficient to fill the spectroelectrochemical cell. Prior to the electrochemical measurements, each sample was mixed with 17 different redox mediators, to a final concentration of 25 μM in each case.[35]

For the electrochemical redox titrations, the spectra were recorded between 200 and −450 mV (Complex I and NADH dehydrogenase fragment) versus the SHE with an interval of 20−30 mV for each step, and the equilibration time was between 15 and 40 min for each point. At the end of each titration, the fully oxidized and fully reduced spectra were compared to the data obtained at the beginning of the experiments to verify the stability of the sample. All potentials described hereafter have been obtained versus Ag/AgCl and then given versus the SHE, by adding 208 mV.

At each potential step, emission spectra were taken with λ_{ex} values of 295, 365, and 420 nm with an integration time of 0.3 s. Analysis of the redox-dependent shift was conducted by taking into account the intensity shift of the signals at 448 and 475 nm, which have been observed in the emission spectra obtained with a λ_{ex} of 420 nm. Then the difference in intensity was plotted versus potential in millivolts (SHE), and the calculation of the midpoint potential was made on the basis of a Nernst fit of the redox transition in the presence of three cofactors.

For the experiments in CH_3CN, the electrochemical cell was adapted to the solvent by changing all materials to Teflon. The reference electrode was replaced by a so-called pseudoreference, including the solution of the quinone as a relative reference and a platinum wire as described previously.[36] The emission spectra were obtained with λ_{ex} values of 365 and 420 nm, and with an integration time of 0.3 s. The difference in the intensity was recorded by applying a potential of −600 mV for the reduced state, and taking 15 successive spectra, doing the same for the oxidation state, and applying a potential of 200 mV. All results were reproducible and fully reversible with an error of ±20 mV, estimated from at least two titrations.

RESULTS AND DISCUSSION

Biochemical Characterization of the Complex I Fragments and the Full Complex. Complex I was prepared from an overproducing strain as reported previously.[29] The complex eluted at 250 mM NaCl from the fractogel anion exchange column and at 260 mM imidazole from the Ni^{2+}-IDA affinity chromatography column. Analytical size exclusion chromatography of the preparation revealed a single peak of the expected size as reported previously.[29] The preparation contained 1.20 ± 0.22 mol of FMN and 1.99 ± 0.34 mol of extractable ubiquinone per mole of complex I. After reconstitution in

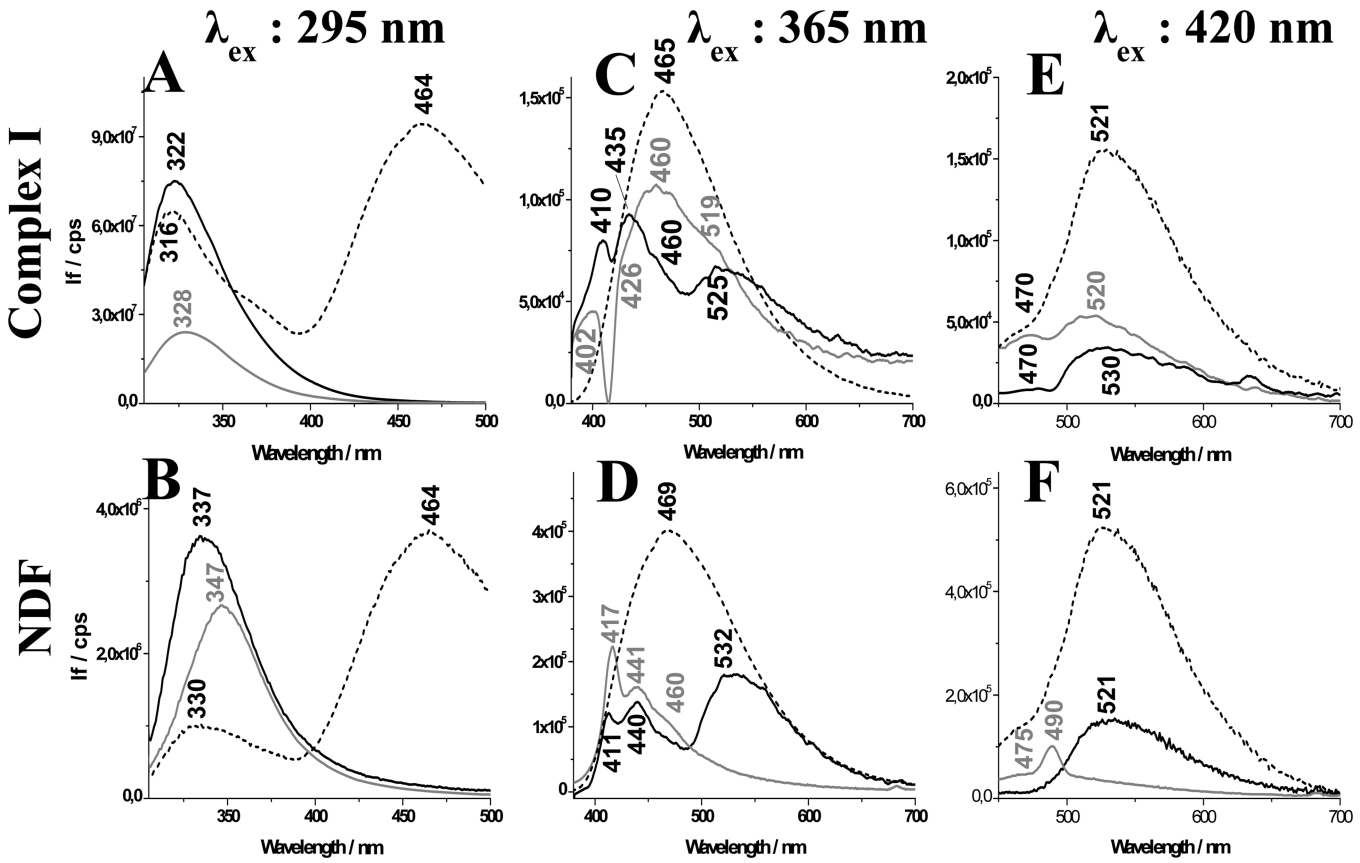

Figure 1. Fluorescence emission spectra of complex I and the NADH dehydrogenase fragment from *E. coli* as isolated (black line), reduced by dithionite (gray line), and reduced by NADH (dashed line). λ_{ex} = 295 nm for panels A and B. λ_{ex} = 365 nm for panels C and D. λ_{ex} = 420 nm for panels E and F.

phospholipids,[37] the preparation catalyzed the NADH:decyl-ubiquinone oxidoreduction with a v_{max} of 2.9 μmol min^{-1} mg^{-1}. This reaction was inhibited by approximately 95% by an addition of 10 μM piericidin A, a specific complex I inhibitor. The K_m^{NADH} was determined to be 13 μM and that for decyl-quinone to be 3 μM.

The NADH dehydrogenase fragment was obtained from an overproducing strain as described previously.[31] The fragment eluted at 160 mM NaCl from a DEAE anion exchange column and was eluted with 2.5 mM D-desthiobiotin from a *Strep*-Tactin Sepharose column.[31] Analytical size exclusion chromatography of the preparation revealed two peaks representing the monomeric and dimeric forms of the preparation. The dimeric form containing all Fe−S clusters in stoichiometric amounts was used for further studies.[31] The preparation contained 1.10 ± 0.12 mol of FMN per mole of protein and no detectable amounts of extractable ubiquinone. The fragment shows the same rate of NADH/ferricyanide oxidoreduction as complex I, namely 80 μmol min^{-1} mg^{-1}, and has the same K_m^{NADH} of 13 μM. However, the fragment exhibits only a very low rate of NADH:decyl-ubiquinone oxidoreduction with a v_{max} of 0.1 μmol min^{-1} mg^{-1} that is not inhibited by piericidin A. The $K_m^{decyl\text{-}quinone}$ of 120 μM is much higher than that of the complex. Thus, the NADH dehydrogenase fragment contains the physiological NADH oxidation site but is missing the quinone reduction site.[30]

The quinone reductase fragment was obtained by splitting the isolated complex at pH 9.[10] The fragment was separated from the NADH dehydrogenase fragment that is also obtained by this treatment by size exclusion chromatography on Bio-Sep-Sec-4000 material. Under the chosen conditions, the NADH dehydrogenase fragment eluted at 65 mL and the quinone reductase fragment at 57 mL corresponding to a molecular mass of ∼720 kDa, thus indicating the dimeric state of the preparation.[10] The quinone reductase fragment showed neither NADH/ferricyanide nor NADH:decyl-ubiquinone oxidoreduction. The preparation contained 1.55 ± 0.22 mol of extractable ubiquinone per mole of protein but no detectable amounts of FMN. Thus, the quinone reductase fragment contains the physiological quinone reduction site but is missing the NADH oxidation site.[10]

Fluorescence Spectra of Complex I and the NADH Dehydrogenase Fragment. Panels A and B of Figure 1 show the fluorescence emission spectra at an excitation wavelength of 295 nm of complex I and the NADH dehydrogenase fragment, respectively. The fluorescence emission of the soluble fragment is seen at 337 nm, a position typical for Trp residues exposed to a polar aqueous environment.[38,39] In complex I, a fluorescence emission signal is seen at 322 nm at a position typical for Trp residues buried in a hydrophobic region.[38,39] Panels C and D of Figure 1 show the fluorescence emission spectra in the spectral range from 400 to 700 nm obtained at an excitation wavelength (λ) of 365 nm. The FMN leads to a signal at 532 nm in the fragment and at 525 nm in complex I. The emission bands at ∼440 nm, in both samples, arise from Trp residues.

The spectra of the same samples reduced by dithionite are shown as gray lines in panels A−F of Figure 1 as obtained at the different excitation wavelengths. The reduction by

dx.doi.org/10.1021/bi4009903 | *Biochemistry* 2013, 52, 8993−9000

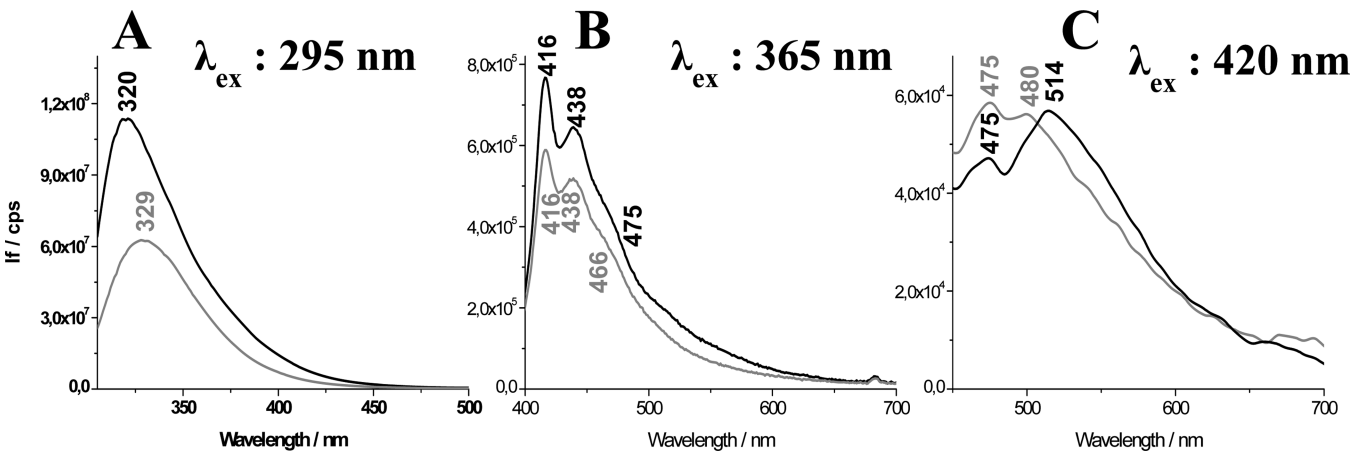

Figure 2. Fluorescence emission spectra of the oxidized (black line) and dithionite-reduced (gray line) NADH dehydrogenase fragment of complex I. λ_{ex} = 295 nm for panel A. λ_{ex} = 365 nm for panel B. λ_{ex} = 420 nm for panel C.

dithionite leads to a decrease in fluorescence intensity and a red-shift of the emission of 7−10 nm. The spectra recorded at an excitation wavelength of 365 or 420 nm show a quenched fluorescence of the FMN due to its reduction.

Via comparison of the spectrum of the reduced complex with that of the reduced NADH dehydrogenase fragment at an excitation wavelength of 365 nm, an additional emission at 460 nm can be detected in the spectrum of complex I (Figure 1C,D, gray lines). This signal is seen as a shoulder in the oxidized form, and its intensity strongly increases in the reduced form. The emission energy indicates that it could arise from the contribution of a quinol or another quinoid chromophore, present in complex I, but not in the soluble fragment.

Finally, the samples were reduced with different concentrations of NADH (Figure 1A−F, dotted lines). In the presence of 500 μM NADH, the Trp fluorescence emission was found to be quenched and blue-shifted by 4 nm (not shown). When the NADH concentration was further increased to >1 mM, the Trp signal was completely quenched. We note that NADH shows a well-known contribution at 464 nm that does not overlap with the protein signals studied here.[40] The spectra obtained at a λ_{ex} of 365 nm are dominated by the NADH emission at 465 nm (Figure 1C,D). The FMN emission observed after addition of NADH in the spectra with a λ_{ex} of 420 nm shifts by 11 nm to 521 nm because of the reduction and the interaction between NADH and the flavin (Figure 1E,F).

Fluorescence Spectra of the Quinone Reductase Fragment. Figure 2 shows the fluorescence emission spectra of the oxidized (black line) and dithionite-reduced (gray line) quinone reductase fragments at three excitation wavelengths (295, 365, and 420 nm). For the λ_{ex} of 295 nm, the fluorescence intensity decreases upon reduction together with a red-shift of the emission peak. With an excitation wavelength of 365 nm, a well-structured fluorescence emission band is observed at 438 nm. The fluorescence band around 416 nm is found to be narrow, most likely because of the superimposition of Raman lines with the emission maximum. In the spectra with a λ_{ex} of 420 nm, two different emission bands at 475 and 514 nm can be distinguished in the reduced form.

In a complementary experiment, the corresponding excitation spectra were analyzed (Figure 3; λ_{em} = 470 nm). A broad excitation band is seen between 330 and 425 nm that red-shifts by 11 nm after reduction from 360 to 371 nm. These signals are characteristic for quinone-like compounds and may include the weak and overlapping bands of quinoid and benzoid $\pi-\pi^*$ transitions.[41−43]

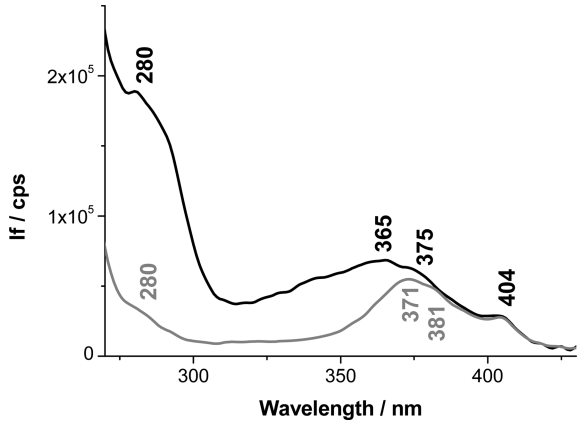

Figure 3. Fluorescence excitation spectra of the oxidized (black line) quinone reductase fragment and the fragment reduced by 500 μM (dark gray line) 1 mM (gray line), or 2 mM dithionite (light gray line) at a λ_{em} of 470 nm.

Fluorescence Spectra of Ubiquinone Radicals. A model compound study was performed to confirm the attribution of the signals by monitoring the reduction of ubiquinone-10 in CH_3CN, an aprotic solvent including residual H_2O in an electrochemical cell by fluorescence spectroscopy. Under these conditions, the formation of the protonated radical can be monitored.[36] The fluorescence emission obtained for a λ_{ex} of 365 nm at 456 nm and for a λ_{ex} of 420 nm at 476 nm (Figure 4A−D) clearly corresponds to the signals seen in complex I and the quinone reductase fragment. These signals are attributed to the increased intensity of the $\pi-\pi^*$ transitions upon reduction.[44]

Electrochemically Induced Fluorescence Analysis of Complex I and the NADH Dehydrogenase Fragment. The redox reactions of complex I and the NADH dehydrogenase fragment were characterized in a thin layer electrochemical cell, specifically adapted for a fluorescence front-face setup.[32] This setup was first extensively tested with cytochrome *c* and then applied to more complex redox proteins.

The electrochemically controlled fluorescence emission spectra of complex I (Figure 5A) and the soluble fragment (Figure 5B) were obtained in the potential range from −450 to

dx.doi.org/10.1021/bi4009903 | *Biochemistry* 2013, 52, 8993−9000

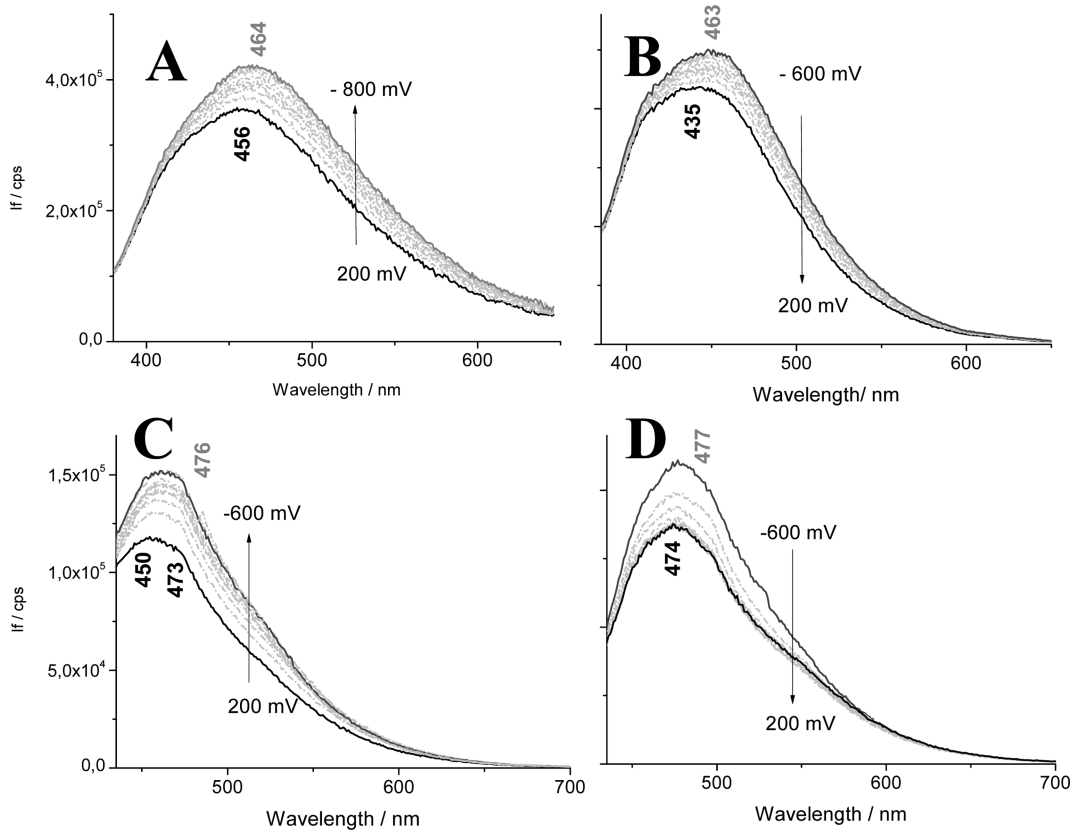

Figure 4. Electrochemically controlled fluorescence emission spectra of ubiquinone in CH_3CN for the potential step from −450 to 200 mV (vs SHE) The fluorescence emission obtained for a λ_{ex} of 365 nm at 456 nm and for a λ_{ex} of 420 nm at 476 nm.

200 mV (vs SHE) using an excitation wavelength of 420 nm. The intensity of the fluorescence emission spectrum increases upon reduction of the enzyme. The emission of the chromophore in question is involved in the large structure at 475 nm in the complex I spectrum. The Nernst fit of the redox-dependent intensity change leads to three redox transitions. The potential at −337 mV (vs SHE) corresponds to the midpoint potential of the FMN cofactor. This result is in line with previous reports and confirms the reliability of the approach.[45,46] Two additional transitions are present at −37 and −235 mV (vs SHE). In the fragment, this redox-dependent change is not detectable and only the change in intensity corroborating the flavin signal can be depicted.

CONCLUSION

The fluorescence emission spectra obtained for complex I and different fragments of the complex indicate the presence of two chromophores with emission at 460 and 475 nm, respectively, and an absorption around 325 nm. The chromophores were reduced by either NADH or dithionite. The electrochemical titration monitored by fluorescence spectroscopy of complex I reveals redox transitions at −37 and −235 mV (vs SHE) indicating the presence of either two compounds with similar spectral properties or two distinct transitions of the same compound. Spectroscopic analysis of the quinone reductase fragment demonstrates that the cofactor(s) is located at the most distal end of the electron transfer chain in accordance with the determined midpoint potentials. As previously reported,[27] complex I contains a NADH-reducible redox group with a midpoint potential above −100 mV that does not appear in the soluble fragment and seems to be the direct electron transfer partner of cluster N2.[47] Because the signals of the chromophores detected in this study show absorbancies in the same spectral area described by Bauscher et al.,[36] we suggest that the redox transition at −100 mV is an average of the two transitions depicted in this study.

On the basis of structural data, the presence of one ubiquinone binding site was reported for complex I.[19] However, two quinone radicals were described by EPR spectroscopy, namely, SQ_{Nf} (fast) and SQ_{Ns} (slow), because of their spin relaxation properties.[16,24−26,48]

We propose that the signals described in this work correspond to mainly SQ_{Ns} due to the fact that the stability of SQ_{Nf} strongly depends of the presence of a proton motive force that is not established in our experiments. The redox potentials of the transitions are in line with the proposal and imply an involvement of SQ_{Nf} in the electron transfer reaction to the pool ubiquinone during the catalytic cycle.[27] EPR studies have determined the distance between N2 and ubiquinone to be 12 Å and place ubiquinone 5 Å within the lipid bilayer.[16] This proposal was confirmed by the recently published structure of the complex.[19] This would imply a location of N2 approximately 7 Å above the membrane. These data suggest that SQ_{Nf} that is sensitive to the presence of a membrane potential is the direct electron acceptor from cluster N2, while SQ_{NS} being insensitive to the presence of a membrane potential works as a converter to transform two one-electron transitions to one two-electron transition as reported for the Q_A/Q_B couple in photosystem II.[49−51] The possibility that complex I works with a modified Q-cycle, as, for example, the bc_1 complex, was excluded for complex I from bovine heart.[52] The authors suggest as a possible explanation for their

dx.doi.org/10.1021/bi4009903 | *Biochemistry* 2013, 52, 8993−9000

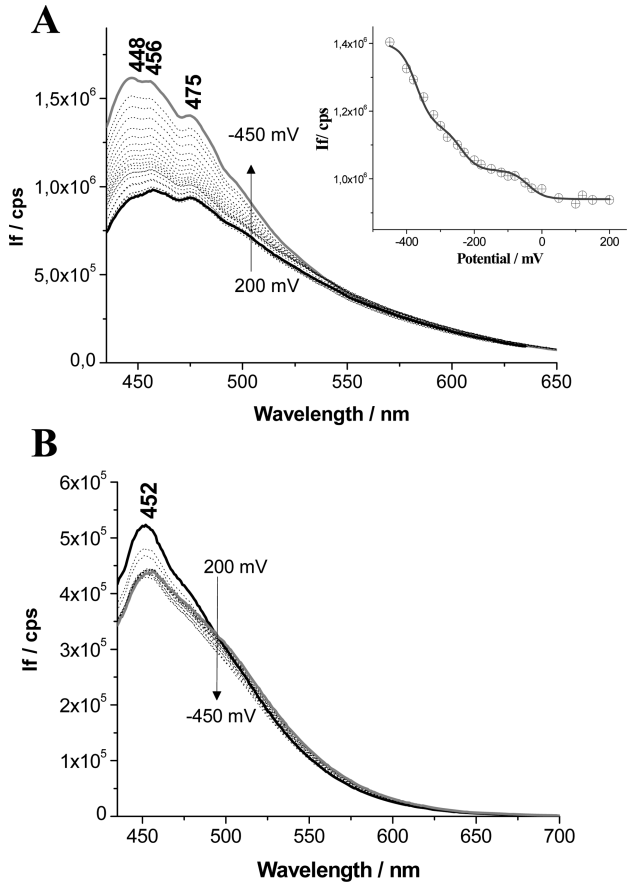

Figure 5. Electrochemically controlled fluorescence emission spectra of complex I for the potential step from −450 to 200 mV (vs SHE) (A). The inset shows the redox-dependent changes monitored at 475 nm. A λ_{ex} of 475 nm shows the electrochemically controlled fluorescence emission spectra of the NADH dehydrogenase fragment for the potential step from −450 to 200 mV (vs SHE) (B).

observations made for the inhibited enzyme a quinone retained in the enzyme and "switched" internally by a second active site. This would require a controlled directional uptake and release of protons from a single large site to alternate sides of the membrane.

In an alternative interpretation, it may be suggested that the signals seen in the fluorescence spectra arise from quinoid cofactors that derive from post-translational modifications of amino acids.[53] However, mass spectrometric analysis of bovine heart complex I subunits revealed no evidence of such post-translational modifications.[54] Together with the observation that ubiquinone in an aprotic solvent shows signals similar to the one detected in complex I, we conclude that the redox transitions described here derive from intermediates of the electron transfer involving two protonated ubiquinone radical species.

AUTHOR INFORMATION

Corresponding Author

*Hellwig Laboratoire de bioelectrochimie et spectroscopie, UMR 7140, CNRS, Université de Strasbourg, 1, rue Blaise Pascal, 67070 Strasbourg, France. E-mail: hellwig@unistra.fr. Phone: 0033 368 851273.

Present Addresses

[§]R.H.: Department of Radiooncology/Medical Physics, Klinikum Darmstadt, Grafenstraße 9, D-64283 Darmstadt, Germany.

[∥]M.V.: Institute of Physical Chemistry, Romanian Academy of Sciences, Ilie Murgulescu, Splaiul, Independentei 202, 060021 Bucharest, Romania.

Funding

We are grateful for the financial support from the Université de Strasbourg, the CNRS, Institut Universitaire de France, and the Centre international aux Recherches de la Chimie in Strasbourg to P.H., M.Y., and M.V. This work was supported by a grant from the Deutsche Forschungsgemeinschaft (DFG) to T.F. in the framework of IRTG 1478.

Notes

The authors declare no competing financial interest.

ABBREVIATIONS

λ_{ex} and λ_{em}, excitation and emission wavelengths, respectively; NDF, NADH:ubiquinone reductase fragment; ROS, reactive oxygen species; SHE, standard hydrogen electrode; SQ, semiquinone radical; Q, quinone; N2−N7, iron sulfur clusters in complex I.

REFERENCES

(1) Weiss, H., Friedrich, T., Hofhaus, G., and Preis, D. (1991) The respiratory-chain NADH dehydrogenase (complex I) of mitochondria. *Eur. J. Biochem. 197*, 563−576.

(2) Weiss, H., and Friedrich, T. (1991) Redox-linked proton translocation by NADH-ubiquinone reductase (complex I). *J. Bioenerg. Biomembr. 23*, 743−754.

(3) Walker, J. E. (1992) The NADH:ubiquinone oxidoreductase (complex I) of respiratory chains. *Q. Rev. Biophys. 25*, 253−324.

(4) Hirst, J., Carroll, J., Fearnley, I. M., Shannon, R. J., and Walker, J. E. (2003) The nuclear encoded subunits of complex I from bovine heart mitochondria. *Biochim. Biophys. Acta 1604*, 135−150.

(5) Carroll, J., Fearnley, I. M., Shannon, R. J., Hirst, J., and Walker, J. E. (2003) Analysis of the subunit composition of complex I from bovine heart mitochondria. *Mol. Cell. Proteomics 2*, 117−126.

(6) Friedrich, T., Steinmuller, K., and Weiss, H. (1995) The proton-pumping respiratory complex I of bacteria and mitochondria and its homologue in chloroplasts. *FEBS Lett. 367*, 107−111.

(7) Yagi, T., Yano, T., Di Bernardo, S., and Matsuno-Yagi, A. (1998) Procaryotic complex I (NDH-1), an overview. *Biochim. Biophys. Acta 1364*, 125−133.

(8) Friedrich, T., and Scheide, D. (2000) The respiratory complex I of bacteria, archaea and eukarya and its module common with membrane-bound multisubunit hydrogenases. *FEBS Lett. 479*, 1−5.

(9) Grigorieff, N. (1998) Three-dimensional structure of bovine NADH:ubiquinone oxidoreductase (complex I) at 22 Å in ice. *J. Mol. Biol. 277*, 1033−1046.

(10) Bottcher, B., Scheide, D., Hesterberg, M., Nagel-Steger, L., and Friedrich, T. (2002) A novel, enzymatically active conformation of the *Escherichia coli* NADH:ubiquinone oxidoreductase (complex I). *J. Biol. Chem. 277*, 17970−17977.

(11) Baranova, E. A., Holt, P. J., and Sazanov, L. A. (2007) Projection structure of the membrane domain of *Escherichia coli* respiratory complex I at 8 Å resolution. *J. Mol. Biol. 366*, 140−154.

(12) Yagi, T., and Matsuno-Yagi, A. (2003) The proton-translocating NADH-quinone oxidoreductase in the respiratory chain: The secret unlocked. *Biochemistry 42*, 2266−2274.

(13) Sazanov, L. A., and Hinchliffe, P. (2006) Structure of the hydrophilic domain of respiratory complex I from *Thermus thermophilus*. *Science 311*, 1430−1436.

(14) Brandt, U., Kerscher, S., Drose, S., Zwicker, K., and Zickermann, V. (2003) Proton pumping by NADH:ubiquinone oxidoreductase. A

redox driven conformational change mechanism? *FEBS Lett. 545*, 9–17.
(15) Sazanov, L. A. (2007) Respiratory complex I: Mechanistic and structural insights provided by the crystal structure of the hydrophilic domain. *Biochemistry 46*, 2275–2288.
(16) Ohnishi, T., and Salerno, J. C. (2005) Conformation-driven and semiquinone-gated proton-pump mechanism in the NADH-ubiquinone oxidoreductase (complex I). *FEBS Lett. 579*, 4555–4561.
(17) Efremov, R. G., Baradaran, R., and Sazanov, L. A. (2010) The architecture of respiratory complex I. *Nature 465*, 441–445.
(18) Efremov, R. G., and Sazanov, L. A. (2012) The coupling mechanism of respiratory complex I: A structural and evolutionary perspective. *Biochim. Biophys. Acta 1817*, 1785–1795.
(19) Baradaran, R., Berrisford, J. M., Minhas, G. S., and Sazanov, L. A. (2013) Crystal structure of the entire respiratory complex I. *Nature 494*, 443–448.
(20) Hunte, C., Zickermann, V., and Brandt, U. (2010) Functional modules and structural basis of conformational coupling in mitochondrial complex I. *Science 329*, 448–451.
(21) Radermacher, M., Ruiz, T., Fowler, D. J., Yu, L., Drose, S., Krack, S., Kerscher, S., Zickermann, V., and Brandt, U. (2011) 3D Reconstruction of a Subcomplex of NADH-ubiquinone-oxidoreductase (Complex I) from *Yarrowia lipolytica*. *Microsc. Microanal. 17*, 90–91.
(22) Pohl, T., Bauer, T., Dorner, K., Stolpe, S., Sell, P., Zocher, G., and Friedrich, T. (2007) Iron-sulfur cluster N7 of the NADH:ubiquinone oxidoreductase (complex I) is essential for stability but not involved in electron transfer. *Biochemistry 46*, 6588–6596.
(23) Berrisford, J. M., Thompson, C. J., and Sazanov, L. A. (2008) Chemical and NADH-induced, ROS-dependent, cross-linking between subunits of complex I from *Escherichia coli* and *Thermus thermophilus*. *Biochemistry 47*, 10262–10270.
(24) Ohnishi, T. (1998) Iron-sulfur clusters/semiquinones in complex I. *Biochim. Biophys. Acta 1364*, 186–206.
(25) Ohnishi, S. T., Salerno, J. C., and Ohnishi, T. (2010) Possible roles of two quinone molecules in direct and indirect proton pumps of bovine heart NADH-quinone oxidoreductase (complex I). *Biochim. Biophys. Acta 1797*, 1891–1893.
(26) Narayanan, M., Gabrieli, D. J., Leung, S. A., Elguindy, M. M., Glaser, C. A., Saju, N., Sinha, S. C., and Nakamaru-Ogiso, E. (2013) Semiquinone and Cluster N6 Signals in His-tagged Proton-translocating NADH:Ubiquinone Oxidoreductase (Complex I) from *Escherichia coli*. *J. Biol. Chem. 288*, 14310–14319.
(27) Friedrich, T., Brors, B., Hellwig, P., Kintscher, L., Rasmussen, T., Scheide, D., Schulte, U., Mantele, W., and Weiss, H. (2000) Characterization of two novel redox groups in the respiratory NADH:ubiquinone oxidoreductase (complex I). *Biochim. Biophys. Acta 1459*, 305–309.
(28) Schulte, U., Abelmann, A., Amling, N., Brors, B., Friedrich, T., Kintscher, L., Rasmussen, T., and Weiss, H. (1998) Search for novel redox groups in mitochondrial NADH:ubiquinone oxidoreductase (complex I) by diode array UV/VIS spectroscopy. *Biofactors 8*, 177–186.
(29) Pohl, T., Uhlmann, M., Kaufenstein, M., and Friedrich, T. (2007) Lambda Red-mediated mutagenesis and efficient large scale affinity purification of the *Escherichia coli* NADH:ubiquinone oxidoreductase (complex I). *Biochemistry 46*, 10694–10702.
(30) Braun, M., Bungert, S., and Friedrich, T. (1998) Characterization of the overproduced NADH dehydrogenase fragment of the NADH:ubiquinone oxidoreductase (complex I) from *Escherichia coli*. *Biochemistry 37*, 1861–1867.
(31) Bungert, S., Krafft, B., Schlesinger, R., and Friedrich, T. (1999) One-step purification of the NADH dehydrogenase fragment of the *Escherichia coli* complex I by means of Strep-tag affinity chromatography. *FEBS Lett. 460*, 207–211.
(32) Voicescu, M., Rother, D., Bardischewsky, F., Friedrich, C. G., and Hellwig, P. (2011) A combined fluorescence spectroscopic and electrochemical approach for the study of thioredoxins. *Biochemistry 50*, 17–24.
(33) Moss, D., Nabedryk, E., Breton, J., and Mantele, W. (1990) Redox-linked conformational changes in proteins detected by a combination of infrared spectroscopy and protein electrochemistry. Evaluation of the technique with cytochrome c. *Eur. J. Biochem. 187*, 565–572.
(34) Hellwig, P., Behr, J., Ostermeier, C., Richter, O. M., Pfitzner, U., Odenwald, A., Ludwig, B., Michel, H., and Mantele, W. (1998) Involvement of glutamic acid 278 in the redox reaction of the cytochrome c oxidase from *Paracoccus denitrificans* investigated by FTIR spectroscopy. *Biochemistry 37*, 7390–7399.
(35) Hellwig, P., Scheide, D., Bungert, S., Mantele, W., and Friedrich, T. (2000) FT-IR spectroscopic characterization of NADH:ubiquinone oxidoreductase (complex I) from *Escherichia coli*: Oxidation of FeS cluster N2 is coupled with the protonation of an aspartate or glutamate side chain. *Biochemistry 39*, 10884–10891.
(36) Bauscher, M., and Maentele, W. (1992) Electrochemical and infrared-spectroscopic characterization of redox reactions of p-quinones. *J. Phys. Chem. 96*, 11101–11108.
(37) Stolpe, S., and Friedrich, T. (2004) The *Escherichia coli* NADH:ubiquinone oxidoreductase (complex I) is a primary proton pump but may be capable of secondary sodium antiport. *J. Biol. Chem. 279*, 18377–18383.
(38) Stryer, L. (1978) Fluorescence energy transfer as a spectroscopic ruler. *Annu. Rev. Biochem. 47*, 819–846.
(39) Lakowicz, J. R. (1999) *Principles of fluorescence spectroscopy*, Kluwer Academic/Plunum Publishers, New York.
(40) Blinova, K., Carroll, S., Bose, S., Smirnov, A. V., Harvey, J. J., Knutson, J. R., and Balaban, R. S. (2005) Distribution of mitochondrial NADH fluorescence lifetimes: Steady-state kinetics of matrix NADH interactions. *Biochemistry 44*, 2585–2594.
(41) Poulsen, J. R., and Birks, J. W. (1989) Photoreduction Fluorescence Detection of quinones in High-Performance Liquid Chromatography. *Anal. Chem. 61*, 2267–2276.
(42) Zhu, Q. Z., Xu, J. G., Guo, X. Q., Zheng, X. Y., Li, W. Y., and Zhao, Y. B. (1997) In-situ photochemical spectrofluorimetric detection of 9,10-anthraquinone-labeled bovine serum albumin. *Spectrochim. Acta, Part A 53A*, 2195–2200.
(43) Cory, R. M., and McKnight, D. M. (2005) Fluorescence spectroscopy reveals ubiquitous presence of oxidized and reduced quinones in dissolved organic matter. *Environ. Sci. Technol. 39*, 8142–8149.
(44) Babaei, A., Connor, P. A., McQuillan, A. J., and Umapathy, S. (1997) UV-visible spectroelectrochemistry of reduction products of anthraquinone in dimethylformamide solutions. *J. Chem. Educ. 74*, 1200–1204.
(45) Sled, V. D., Rudnitzky, N. I., Hatefi, Y., and Ohnishi, T. (1994) Thermodynamic analysis of flavin in mitochondrial NADH:ubiquinone oxidoreductase (complex I). *Biochemistry 33*, 10069–10075.
(46) Birrell, J. A., Yakovlev, G., and Hirst, J. (2009) Reactions of the flavin mononucleotide in complex I: A combined mechanism describes NADH oxidation coupled to the reduction of $APAD^+$, ferricyanide, or molecular oxygen. *Biochemistry 48*, 12005–12013.
(47) Duarte, M., Populo, H., Videira, A., Friedrich, T., and Schulte, U. (2002) Disruption of iron-sulphur cluster N2 from NADH:ubiquinone oxidoreductase by site-directed mutagenesis. *Biochem. J. 364*, 833–839.
(48) Ohnishi, T., Ohnishi, S. T., Shinzawa-Itoh, K., Yoshikawa, S., and Weber, R. T. (2012) EPR detection of two protein-associated ubiquinone components (SQ_{Nf} and SQ_{Ns}) in the membrane in situ and in proteoliposomes of isolated bovine heart complex I. *Biochim. Biophys. Acta 1817*, 1803–1809.
(49) Minagawa, J., Narusaka, Y., Inoue, Y., and Satoh, K. (1999) Electron Transfer between Q_A and Q_B in Photosystem II Is Thermodynamically Perturbed in Phototolerant Mutants of *Synechocystis* sp. PCC 6803. *Biochemistry 38*, 770–775.
(50) Boussac, A., Sugiura, M., and Rappaport, F. (2011) Probing the quinone binding site of Photosystem II from *Thermosynechococcus elongatus* containing either PsbA1 or PsbA3 as the D1 protein through the binding characteristics of herbicides. *Biochim. Biophys. Acta 1807*, 119–129.

(51) de Wijn, R., and van Gorkom, H. J. (2001) Kinetics of Electron Transfer from QA to QB in Photosystem II. *Biochemistry 40*, 11912−11922.
(52) Sherwood, S., and Hirst, J. (2006) Investigation of the mechanism of proton translocation by NADH:ubiquinone oxidoreductase (complex I) from bovine heart mitochondria: Does the enzyme operate by a Q-cycle mechanism? *Biochem. J. 400*, 541−550.
(53) Reddy, S. Y., and Bruice, T. C. (2004) Determination of enzyme mechanisms by molecular dynamics: Studies on quinoproteins, methanol dehydrogenase, and soluble glucose dehydrogenase. *Protein Sci. 13*, 1965−1978.
(54) Carroll, J., Fearnley, I. M., Wang, Q., and Walker, J. E. (2009) Measurement of the molecular masses of hydrophilic and hydrophobic subunits of ATP synthase and complex I in a single experiment. *Anal. Biochem. 395*, 249−255.